

## Parameter Estimation for Balance-Equal Replicated Linear Functional Relationship Model: An Application to the Wind Directional Data

Mohd Faisal Saari<sup>1\*</sup>, Abdul Ghapor Hussin<sup>2</sup>, Yong Zulina Zubairi<sup>3</sup> & Mohd Syazwan Mohamad Anuar<sup>1</sup>

<sup>1</sup>*Centre for Defence Foundation Studies, Universiti Pertahanan Nasional Malaysia, 57000 Kuala Lumpur, Malaysia*

<sup>2</sup>*Faculty of Defence Science and Technology, Universiti Pertahanan Nasional Malaysia, 57000 Kuala Lumpur, Malaysia.*

<sup>3</sup>*Centre for Foundation Studies in Science, Universiti Malaya, 50603 Kuala Lumpur, Malaysia.*

*\*Corresponding author: mohdfaisal37@gmail.com*

### Abstract

A linear functional relationship model can be used to model the relationship between two circular variables when both variables are observed with errors. When the ratio of error concentration parameter is unknown, it is suggested that the replicated linear functional relationship model be used. The purpose of this paper is to present all the parameter estimates of the replicated linear functional relationship model for balance replicates and equal circular variables. Simulations studies are performed to understand the behavior of the parameter estimators for the balance-equal replicated linear functional relationship model. The empirical results obtained suggest that the proposed parameter estimation method performs well with small bias. A simple application of the model is demonstrated by analyzing a real dataset of a wind directional data.

**Keywords:** Circular Variables, Linear Functional Relationship Model, Parameter Estimation, Replicated, Wind Direction

### 1. Introduction

The unidentifiability problem in an unreplicated linear functional relationship model (LFRM) can be avoided if the ratio of error concentration parameter  $\lambda$  is known in order to estimate the parameters (Mokhtar et al., 2017). However, the value  $\lambda$  is unknown in most actual circumstances because the information is either unavailable or not provided by field researchers. One essential strategy to avoid this difficulty is to collect this information from the sample itself (Arif et al., 2020b). This is accomplished by recognizing groups of pseudo-replicates from unreplicated linear data in which all parameters are identifiable and reliably approximated (Hussin et al., 2004). Furthermore, the replicated

LFRM can be employed by replicating observations from unreplicated data or by making replication available. The replicated LFRM can be utilized to avoid the LFRM's unidentifiability problem. Furthermore, since the error concentration parameter for  $X_i$  variable ( $\kappa_x$ ) and error concentration parameter for  $Y_i$  variable ( $\kappa_y$ ) can be estimated separately using replicated LFRM, the assumption or knowledge on the ratio of the error concentration parameter is no longer required. Practical applications can be seen in many fields such as meteorology (Moslim et al., 2021), psychopathology (Hinton et al., 2018), physical recovery (Hannanu et al., 2020), genetic networks (Selvaggi et al., 2019) and Parkinson diagnostic (Goetz et al., 2019)

Assume that each group has the same size, which implies that the observations or components in each group are the same. This is referred to as balance and equal replicates, where measurements  $x_{ij}$  ( $j=1,2,\dots,m_i$ ) are made on  $X_i$  and measurements  $y_{ik}$  ( $k=1,2,\dots,m_i$ ) are made on  $Y_i$  are equal ( $j=k=1,2,\dots,m_i$ ). There may be replicated observations of  $X_i$  and  $Y_i$  occurring in  $p$  groups given a certain pair  $(X_i, Y_i)$  and  $i=1,2,\dots,p$ . In this paper, we extended the works of Mokhtar et al. (2017), to derive all the parameter estimates of the model.

## 2. Balance-Equal Replicated Linear Functional Relationship Model

As mentioned earlier, the balance-equal replicated LFRM is an extension of the unreplicated LFRM. Corresponding to a particular pair  $(X_i, Y_i)$  there may be replicated observations of  $X_i$  and  $Y_i$  occurring in  $p$  groups. Suppose  $x_{ij}$  and  $y_{ik}$  are observed values of the circular variables  $X_i$  and  $Y_i$  respectively, thus  $0 \leq x_{ij}, y_{ik} \leq 2\pi$  for  $i=1,2,\dots,p$ ,  $j=1,2,\dots,m_i$  and  $k=1,2,\dots,m_i$ . For any fixed  $X_i$  and  $Y_i$ , noted that the observations  $x_{ij}$  and  $y_{ik}$  have been measured with errors  $\delta_i$  and  $\varepsilon_i$  respectively.

By assuming  $\alpha$  as rotation parameter and  $\beta$  as slope parameter, the balance-equal replicated LFRM can be written as

$$\begin{aligned} x_{ij} &= X_i + \delta_{ij}, & y_{ik} &= Y_i + \varepsilon_{ik} \\ Y_i &= \alpha + \beta X_i \pmod{2\pi} \end{aligned} \quad (1)$$

for  $i=1,2,\dots,p$ ,  $j=1,2,\dots,m_i$  and  $k=1,2,\dots,m_i$

where  $\delta_i$  and  $\varepsilon_i$  are homogeneous and independently distributed by von Mises distributions with zero mean circular, that is  $\delta_i \sim VM(0, \kappa_x)$  and  $\varepsilon_i \sim VM(0, \kappa_y)$  where  $\kappa_x$  is error concentration parameter for  $X_i$  variable and  $\kappa_y$  is error concentration parameter for  $Y_i$  variable.

There are  $(p+4)$  parameters that need to be estimated by using maximum likelihood estimation  $\hat{\alpha}, \hat{\beta}, \hat{\kappa}_x, \hat{\kappa}_y$  and the incidental parameters  $\hat{X}_i$ . Note that in unreplicated LFRM the ratio of error

concentration parameter  $\lambda$  was needed to estimate the concentration parameters of  $\kappa_x$  and  $\kappa_y$ . However, in replicated LFRM the ratio of error concentration parameter is unnecessary.

Von Mises distribution is one of the finest for describing circle distribution (Kamisan et al., 2010). The probability density function of the von Mises distribution is provided for every circular random variable  $\theta$  with mean direction  $\mu$  and concentration parameter  $\kappa$  as,

$$g(\mu, \kappa; \theta) = \frac{1}{2\pi I_0(\kappa)} \exp\{\kappa \cos(\theta - \mu)\}$$

where  $I_0(\kappa) = \frac{1}{2\pi} \int_0^{2\pi} \exp\{\kappa \cos \theta\} d\theta$  is defined as the modified Bessel function of the first kind and order zero. The von Mises distribution's log-likelihood function can be represented by

$$\begin{aligned} \log L(\alpha, \beta, \kappa_x, \kappa_y, X_i; x_{ij}, y_{ik}) &= -NM \log(2\pi) - N \log I_0(\kappa_x) \\ &- M \log I_0(\kappa_y) + \kappa_x \sum_{i=1}^p \sum_{j=1}^m \cos(x_{ij} - X_i) + \kappa_y \sum_{i=1}^p \sum_{k=1}^m \cos(y_{ik} - \alpha - \beta X_i) \end{aligned} \quad (2)$$

where  $N$  is the total sample size of  $x_{ij}$  and  $M$  is the total sample size of  $y_{ik}$ .

### 3. Parameter Estimation Using Maximum Likelihood Estimation

All estimated parameters can be derived by differentiating Equation (2) with respect to respective parameters.

#### i. Parameter estimation for the rotation parameter

The first partial derivatives of Equation (2) with respect to  $\alpha$  is

$$\frac{\partial \log L}{\partial \alpha} = \kappa_y \sum_{i=1}^p \sum_{k=1}^m \sin(y_{ik} - \alpha - \beta X_i)$$

Setting this equal to zero and simplifying

$$\sum_{i=1}^p \sum_{k=1}^m \sin(y_{ik} - \hat{\beta} \hat{X}_i) \cos \hat{\alpha} - \sum_{i=1}^p \sum_{k=1}^m \cos(y_{ik} - \hat{\beta} \hat{X}_i) \sin \hat{\alpha} = 0$$

Solving for  $\hat{\alpha}$

$$\begin{aligned} \tan \hat{\alpha} &= \frac{\sum_{i=1}^p \sum_{k=1}^m \sin(y_{ik} - \hat{\beta} \hat{X}_i)}{\sum_{i=1}^p \sum_{k=1}^m \cos(y_{ik} - \hat{\beta} \hat{X}_i)} \\ \hat{\alpha} &= \tan^{-1} \left[ \frac{\sum_{i=1}^p \sum_{k=1}^m \sin(y_{ik} - \hat{\beta} \hat{X}_i)}{\sum_{i=1}^p \sum_{k=1}^m \cos(y_{ik} - \hat{\beta} \hat{X}_i)} \right] \end{aligned}$$

Let  $\hat{\alpha} = \tan^{-1}\left(\frac{S}{C}\right)$ , where  $S = \sum_{i=1}^p \sum_{k=1}^m \sin(y_{ik} - \hat{\beta} \hat{X}_i)$  and  $C = \sum_{i=1}^p \sum_{k=1}^m \cos(y_{ik} - \hat{\beta} \hat{X}_i)$ . Then

$$\hat{\alpha} = \begin{cases} \tan^{-1}\left(\frac{S}{C}\right), & S > 0, C > 0 \\ \tan^{-1}\left(\frac{S}{C}\right) + \pi, & C < 0 \\ \tan^{-1}\left(\frac{S}{C}\right) + 2\pi, & S < 0, C > 0 \end{cases} \quad (3)$$

### ii. Parameter estimation for the slope parameter

The first partial derivatives of Equation (2) with respect to  $\beta$  is

$$\frac{\partial \log L}{\partial \beta} = \kappa_y \sum_{i=1}^p \sum_{k=1}^m X_i \sin(y_{ik} - \alpha - \beta X_i)$$

Setting this equal to zero and simplifying

$$\sum_{i=1}^p \sum_{k=1}^m \hat{X}_i \sin(y_{ik} - \hat{\alpha} - \hat{\beta} \hat{X}_i) = 0$$

Iteratively, the expected slope parameter can be obtained using Newton-Raphson iteration approach. Assume  $\hat{\beta}_0$  is an early estimate of  $\hat{\beta}$  and  $\hat{\beta}_1$  is an improvement of  $\hat{\beta}_0$ , estimation using the iteration method yields

$$\hat{\beta}_1 \approx \hat{\beta}_0 + \frac{\sum_{i=1}^p \sum_{k=1}^m \hat{X}_i \sin(y_{ik} - \hat{\alpha} - \hat{\beta}_0 \hat{X}_i)}{\sum_{i=1}^p \sum_{k=1}^m \hat{X}_i^2 \cos(y_{ik} - \hat{\alpha} - \hat{\beta}_0 \hat{X}_i)} \quad (4)$$

### iii. Parameter estimation for concentration parameter for $X$ variable

The first partial derivatives of Equation (2) with respect to  $\kappa_x$  is

$$\frac{\partial \log L}{\partial \kappa_x} = -N \frac{I_0'(\kappa_x)}{I_0(\kappa_x)} + \sum_{i=1}^p \sum_{j=1}^m \cos(x_{ij} - X_i) = -NA(\kappa_x) + \sum_{i=1}^p \sum_{j=1}^m \cos(x_{ij} - X_i)$$

where  $A(\kappa_x) = \frac{I_0'(\kappa_x)}{I_0(\kappa_x)} = \frac{I_1(\kappa_x)}{I_0(\kappa_x)}$ ,  $I_0(\kappa_x)$  and  $I_1(\kappa_x)$  are the asymptotic power series for Bessel

function. Setting this equal to zero and simplifying

$$\begin{aligned} -NA(\hat{\kappa}_x) + \sum_{i=1}^p \sum_{j=1}^m \cos(x_{ij} - \hat{X}_i) &= 0 \\ A(\hat{\kappa}_x) &= \frac{1}{N} \left[ \sum_{i=1}^p \sum_{j=1}^m \cos(x_{ij} - \hat{X}_i) \right] \end{aligned}$$

The estimation of  $\hat{\kappa}_x$  can be obtained by using the Dobson's approximation (Dobson, 1978),

$$A^{-1}(w) = \frac{9 - 8w + 3w^2}{8(1 - w)}$$

Therefore,

$$\hat{\kappa}_x = A^{-1}\{w\} \text{ where } w = \frac{1}{N} \left[ \sum_{i=1}^p \sum_{j=1}^m \cos(x_{ij} - \hat{X}_i) \right] \quad (5)$$

#### iv. Parameter estimation for concentration parameter for Y variable

The first partial derivatives of Equation (2) with respect to  $\kappa_y$  is

$$\frac{\partial \log L}{\partial \kappa_y} = -M \frac{I_0'(\kappa_y)}{I_0(\kappa_y)} + \sum_{i=1}^p \sum_{k=1}^m \cos(y_{ik} - \alpha - \beta X_i) = -MA(\kappa_y) + \sum_{i=1}^p \sum_{k=1}^m \cos(y_{ik} - \alpha - \beta X_i)$$

where  $A(\kappa_y) = \frac{I_0'(\kappa_y)}{I_0(\kappa_y)} = \frac{I_1(\kappa_y)}{I_0(\kappa_y)}$ ,  $I_0(\kappa_y)$  and  $I_1(\kappa_y)$  are the asymptotic power series for Bessel

function. Setting this equal to zero and simplifying

$$\begin{aligned} -MA(\hat{\kappa}_y) + \sum_{i=1}^p \sum_{k=1}^m \cos(y_{ik} - \hat{\alpha} - \hat{\beta} \hat{X}_i) &= 0 \\ A(\hat{\kappa}_y) &= \frac{1}{M} \left[ \sum_{i=1}^p \sum_{k=1}^m \cos(y_{ik} - \hat{\alpha} - \hat{\beta} \hat{X}_i) \right] \end{aligned}$$

The estimation of  $\hat{\kappa}_y$  can also be obtained by using the Dobson approximation. Therefore,

$$\hat{\kappa}_y = A^{-1}\{w\} \text{ where } w = \frac{1}{M} \left[ \sum_{i=1}^p \sum_{k=1}^m \cos(y_{ik} - \hat{\alpha} - \hat{\beta} \hat{X}_i) \right] \quad (6)$$

#### v. Parameter estimation for incidental parameters

The first partial derivatives of Equation (2) with respect to  $X_i$  is

$$\frac{\partial \log L}{\partial X_i} = \kappa_x \sum_{j=1}^m \sin(x_{ij} - X_i) + \kappa_y \beta \sum_{k=1}^m \sin(y_{ik} - \alpha - \beta X_i)$$

Setting this equal to zero and simplifying

$$\hat{\kappa}_x \sum_{j=1}^m \sin(x_{ij} - \hat{X}_i) + \hat{\kappa}_y \hat{\beta} \sum_{k=1}^m \sin(y_{ik} - \hat{\alpha} - \hat{\beta} \hat{X}_i) = 0$$

Assume  $\hat{X}_{i0}$  is an early estimate of  $\hat{X}_i$  and  $\hat{X}_{i1}$  is an improvement of  $\hat{X}_{i0}$ , estimation of  $\hat{X}_i$  using the Newton-Raphson iteration method gives

$$\hat{X}_{i1} = \hat{X}_{i0} + \frac{\hat{\kappa}_x \sum_{j=1}^m \sin(x_{ij} - \hat{X}_{i0}) + \hat{\kappa}_y \hat{\beta} \sum_{k=1}^m \sin(y_{ik} - \hat{\alpha} - \hat{\beta} \hat{X}_{i0})}{\hat{\kappa}_x \sum_{j=1}^m \cos(x_{ij} - \hat{X}_{i0}) + \hat{\kappa}_y \hat{\beta}^2 \sum_{k=1}^m \cos(y_{ik} - \hat{\alpha} - \hat{\beta} \hat{X}_{i0})} \quad (7)$$

**vi. Variance of the parameters**

The estimated variance of parameters can be determined using several approximations (Hussin et al., 2010) and the Fisher information matrix (Satari et al., 2014). It can be demonstrated that the variance of parameters are,

$$\begin{aligned} \hat{V}ar(\hat{\alpha}) &= \frac{p \left[ \hat{\kappa}_x MA(\hat{\kappa}_x) + \hat{\kappa}_y N \hat{\beta}^2 A(\hat{\kappa}_y) \right] \sum_{i=1}^p \hat{X}_i^2}{\left[ \hat{\kappa}_x MA(\hat{\kappa}_x) \hat{\kappa}_y NA(\hat{\kappa}_y) \right] \left[ p \sum_{i=1}^p \hat{X}_i^2 - \left( \sum_{i=1}^p \hat{X}_i \right)^2 \right]} \\ \hat{V}ar(\hat{\beta}) &= \frac{p^2 \left[ \hat{\kappa}_x MA(\hat{\kappa}_x) + \hat{\kappa}_y N \hat{\beta}^2 A(\hat{\kappa}_y) \right]}{\left[ \hat{\kappa}_x MA(\hat{\kappa}_x) \hat{\kappa}_y NA(\hat{\kappa}_y) \right] \left[ p \sum_{i=1}^p \hat{X}_i^2 - \left( \sum_{i=1}^p \hat{X}_i \right)^2 \right]} \\ \hat{V}ar(\hat{\kappa}_x) &= \frac{\hat{\kappa}_x}{M \hat{\kappa}_x - M \hat{\kappa}_x A^2(\hat{\kappa}_x) - MA(\hat{\kappa}_x)} \\ \hat{V}ar(\hat{\kappa}_y) &= \frac{\hat{\kappa}_y}{N \hat{\kappa}_y - N \hat{\kappa}_y A^2(\hat{\kappa}_y) - NA(\hat{\kappa}_y)} \end{aligned}$$

**4. Simulation Study**

In order to validate the accuracy of the estimation parameters in this suggested model, a Monte Carlo simulation analysis was performed. For each set of simulations, the number of simulations ( $s$ ) is set to 5000. Without sacrificing generality, consider the true values of  $\alpha = \pi/4$  and  $\beta = 1$ , whereas the equivalent values of  $(\kappa_x, \kappa_y) = (5,5), (10,10), (15,15)$  are also considered into the simulation. The set of variables  $X$  was generated using the von Mises distribution  $X \sim VM(\pi/4,5)$ , and the sample size  $n = 50, 100, 200, 500$  was taken into account for the simulation.

To simulate the balance-equal replicated environment of circular data, each sample size will be grouped through the pseudo-replicate method as shown in Table 1. Sample size are divided into  $p$  groups. These groups contain  $m$  elements such that  $p \times m = N$  where  $m_i$  is the maximum divisor of  $N$  such that  $p \leq m$  (Arif et al., 2020a).

**Table 1.** Grouping sample size into their corresponding group

| Sample size ( $n$ ) | Number of groups ( $p$ ) | Number of members in each groups ( $m$ ) |
|---------------------|--------------------------|--|
| 50                  | 5                        | 10                                       |
| 100                 | 10                       | 10                                       |
| 200                 | 10                       | 20                                       |
| 500                 | 20                       | 25                                       |

#### 4.1 Biasness of $\alpha$

The rotation parameter is classified as a directional parameter. As a result, three measurements can be used to verify  $\hat{\alpha}$ .

##### i. Circular mean

$$\bar{\hat{\alpha}} = \begin{cases} \tan^{-1}\left(\frac{S}{C}\right) & S > 0, C > 0 \\ \tan^{-1}\left(\frac{S}{C}\right) + \pi & C < 0 \\ \tan^{-1}\left(\frac{S}{C}\right) + 2\pi & S < 0, C > 0 \end{cases}$$

where  $S = \sum_{j=1}^s \sin(\hat{\alpha}_j)$  and  $C = \sum_{j=1}^s \cos(\hat{\alpha}_j)$

##### ii. Circular distance, $d = \pi - \left| \pi - \left| \bar{\hat{\alpha}} - \alpha \right| \right|$

##### iii. Mean resultant length, $\bar{R} = \frac{1}{s} \sqrt{\left( \sum_{j=1}^s \cos(\hat{\alpha}_j) \right)^2 + \left( \sum_{j=1}^s \sin(\hat{\alpha}_j) \right)^2}$

#### 4.2 Biasness of $\beta$ , $\kappa_x$ and $\kappa_y$

The slope parameter and concentration parameter are labelled as the continuous parameter for this proposed model (Arif et al., 2020a). By assuming  $\omega$  as a generic term of  $\beta$ ,  $\kappa_x$  and  $\kappa_y$ , these estimated parameters can be verified using these three methods.

##### i. Mean, $\bar{\hat{\omega}} = \frac{1}{s} \sum_{j=1}^s \hat{\omega}_j$

##### ii. Estimated bias, $EB = \bar{\hat{\omega}} - \omega$

##### iii. Estimated root mean square errors, $ERMSE = \sqrt{\frac{1}{s} \sum_{j=1}^s (\hat{\omega}_j - \omega)^2}$

### 5. Simulation Result

The biasness performance indicator is shown in Table 2 for all parameters. The circular mean approaches the true value of  $\pi/4$  as the sample size ( $n$ ) for each fixed value  $\kappa$  rises, according to Table 2. Similarly, for any fixed  $\kappa$ , the estimation of  $\hat{\alpha}$  improves as  $n$  increases because the circular distance reduces and approaches zero, while the value of the mean resultant length approaches one. This result can also be demonstrated, as seen in Figure 1(a) and Figure 1(b), respectively. Based on these simulation findings, it appears that a good parameter estimation was accomplished.

**Table 2:** Simulation result for all expected parameters

| $\kappa$                           | $n$ | Performance indicator for $\hat{\alpha}$ |        |           | Performance indicator for $\hat{\beta}$ |        |         | Performance indicator for $\hat{\kappa}_x$ |        |         | Performance indicator for $\hat{\kappa}_y$ |        |         |
|------------------------------------|-----|--|--------|-----------|---|--------|---------|--|--------|---------|--|--------|---------|
|                                    |     | Circular Mean                            | $d$    | $\bar{R}$ | Mean                                    | $EB$   | $ERMSE$ | Mean                                       | $EB$   | $ERMSE$ | Mean                                       | $EB$   | $ERMSE$ |
| $\kappa_x = 5$<br>$\kappa_y = 5$   | 50  | 0.6891                                   | 0.0963 | 0.9335    | 1.2896                                  | 0.2896 | 1.9384  | 5.5603                                     | 0.5603 | 1.3310  | 5.5195                                     | 0.5195 | 1.3252  |
|                                    | 100 | 0.7107                                   | 0.0747 | 0.9679    | 1.2553                                  | 0.2552 | 1.4270  | 5.2921                                     | 0.2921 | 0.8336  | 5.2850                                     | 0.2850 | 0.8652  |
|                                    | 200 | 0.7494                                   | 0.0360 | 0.9871    | 1.1137                                  | 0.1137 | 1.1087  | 5.1779                                     | 0.1779 | 0.5688  | 5.1813                                     | 0.1813 | 0.6036  |
|                                    | 500 | 0.7722                                   | 0.0132 | 0.9974    | 1.0382                                  | 0.0382 | 0.7521  | 5.0948                                     | 0.0948 | 0.3598  | 5.1003                                     | 0.1003 | 0.3646  |
| $\kappa_x = 10$<br>$\kappa_y = 10$ | 50  | 0.7369                                   | 0.0485 | 0.9786    | 1.1311                                  | 0.1311 | 1.6875  | 11.2023                                    | 1.2023 | 2.7189  | 11.1883                                    | 1.1883 | 2.7832  |
|                                    | 100 | 0.7489                                   | 0.0365 | 0.9907    | 1.1135                                  | 0.1135 | 0.9077  | 10.6886                                    | 0.6886 | 1.7228  | 10.7007                                    | 0.7007 | 1.7719  |
|                                    | 200 | 0.7643                                   | 0.0211 | 0.9942    | 1.0776                                  | 0.0776 | 0.5217  | 10.4388                                    | 0.4388 | 1.2328  | 10.4381                                    | 0.4381 | 1.2822  |
|                                    | 500 | 0.7767                                   | 0.0087 | 0.9992    | 1.0342                                  | 0.0342 | 0.4213  | 10.2629                                    | 0.2629 | 0.7214  | 10.2711                                    | 0.2711 | 0.7360  |
| $\kappa_x = 15$<br>$\kappa_y = 15$ | 50  | 0.7563                                   | 0.0291 | 0.9867    | 1.0745                                  | 0.0745 | 1.0153  | 16.8072                                    | 1.8072 | 4.0673  | 16.8399                                    | 1.8399 | 4.2436  |
|                                    | 100 | 0.7643                                   | 0.0211 | 0.9944    | 1.0880                                  | 0.0880 | 0.6533  | 16.0213                                    | 1.0213 | 2.5854  | 15.9848                                    | 0.9848 | 2.6412  |
|                                    | 200 | 0.7710                                   | 0.0144 | 0.9973    | 1.0625                                  | 0.0625 | 0.4162  | 15.6492                                    | 0.6492 | 1.7623  | 15.6859                                    | 0.6859 | 1.8453  |
|                                    | 500 | 0.7778                                   | 0.0076 | 0.9993    | 1.0310                                  | 0.0310 | 0.1907  | 15.4053                                    | 0.4053 | 1.0975  | 15.3968                                    | 0.3968 | 1.1310  |



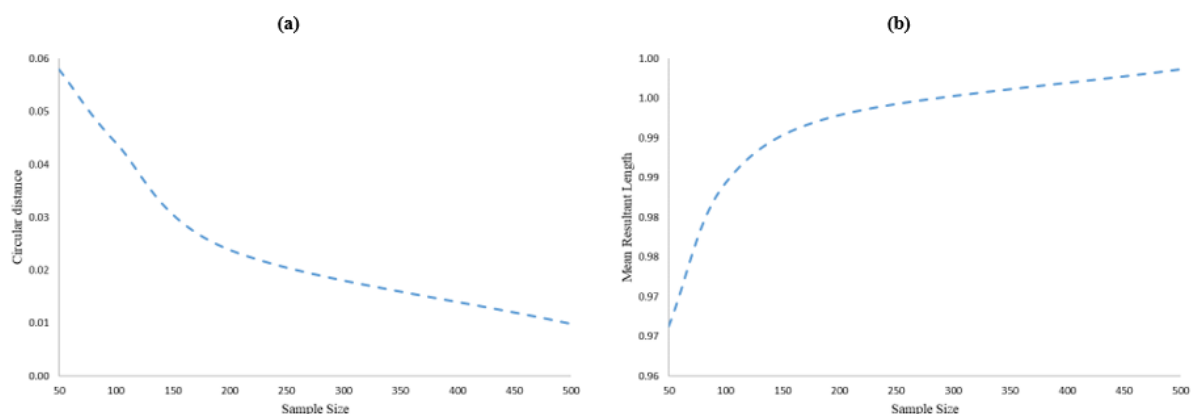


**Figure 1. (a)** Circular distance for  $\hat{\alpha}$  and **(b)** Mean resultant length for  $\hat{\alpha}$

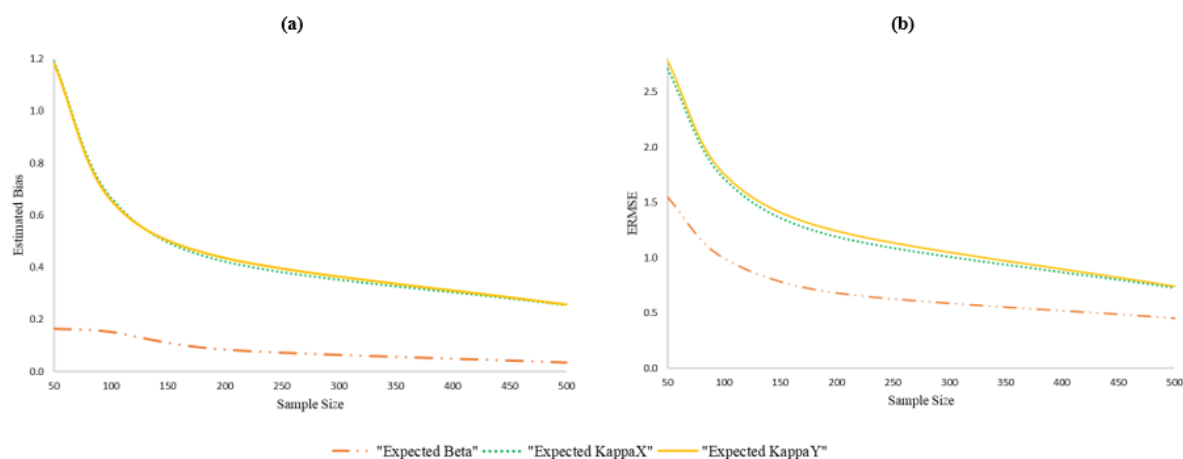


**Figure 2. (a)** Estimated bias for  $\hat{\beta}$ ,  $\hat{\kappa}_x$  and  $\hat{\kappa}_y$  **(b)** ERMSE for  $\hat{\beta}$ ,  $\hat{\kappa}_x$  and  $\hat{\kappa}_y$

A similar conclusion may be drawn by referring to Table 2 and focusing on parameter  $\hat{\beta}$ ,  $\hat{\kappa}_x$  and  $\hat{\kappa}_y$ , where based on these simulation findings, it implies that a good prediction for parameter  $\hat{\beta}$ ,  $\hat{\kappa}_x$  and  $\hat{\kappa}_y$  has also been performed. As the sample size for each fixed  $\kappa$  value increases, the estimated bias (EB) and estimated root mean square errors (ERMSE) for  $\hat{\beta}$ ,  $\hat{\kappa}_x$  and  $\hat{\kappa}_y$  lessen and approach zero, while the mean values for each parameter approach their true value. These conclusions are further supported by Figure 2(a) and Figure 2(b).

Based on the simulation performances, it is possible to conclude that the suggested model is adequate for modelling circular data with very little bias in general. In contrast to the earlier study of replicated functional model by Mokhtar et al. (2017), this proposed replicated linear functional relationship model is able to estimate the parameters without having to assume the ratio of the error concentration parameter and it considers all parameters involved

## 6. Application to Wind Direction

The applicability of the suggested model in this research can be demonstrated by using wind direction data gathered from the Humberside shore of the North Sea in the United Kingdom. With a sample size of 120, the wind direction data acquired by the HF radar system created by UK Rutherford and Appleton Laboratories is treated as the variable  $x_{ij}$ . Meanwhile, the variable  $y_{ik}$  represents wind data collected by an anchored wave buoy.

To apply the balance-equal replicated linear functional relationship model to these data, the data will be replicated based on the period of data collection and grouped into 10 different groups, each with 12 members to generate the balance-equal replicated data. The data will next be simulated into the proposed model.

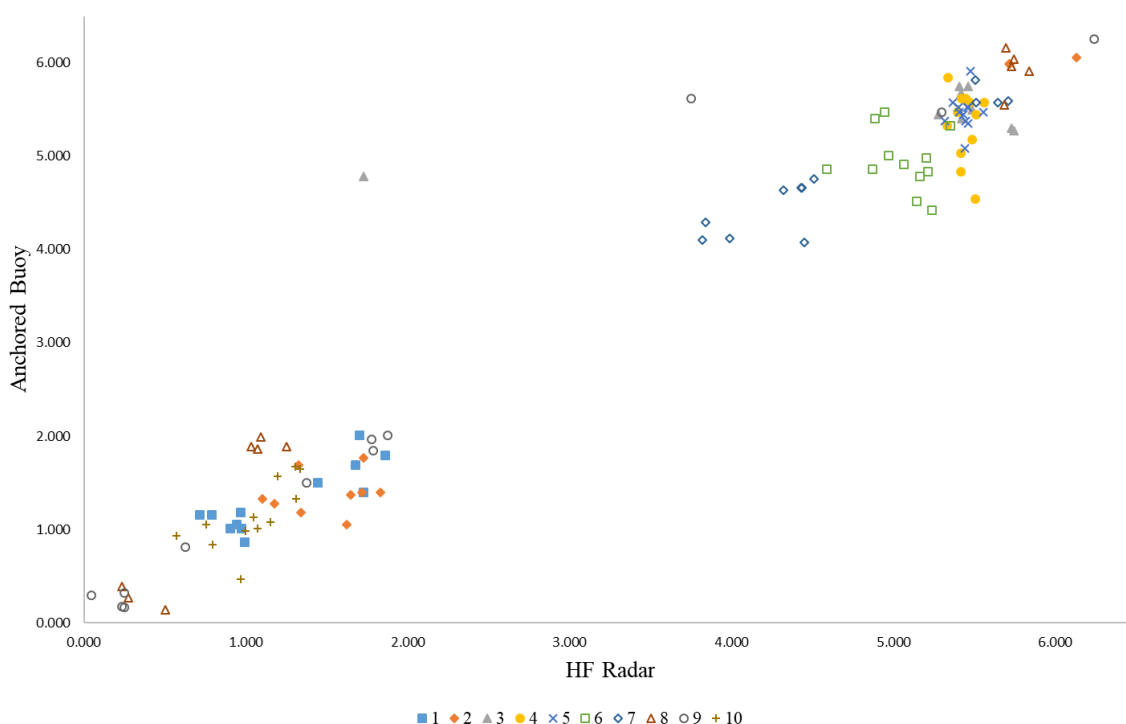


**Figure 3.** Scatter plot of HF radar (x) and anchored buoy (y)

The underlying link between the variables  $x_{ij}$  and  $y_{ik}$  based on the simulation results is given by  $(\text{Anchored Buoy}) = 0.0367 + 0.9927(\text{HF Radar}) \pmod{2\pi}$ , where  $\delta_{ij} \sim VM(0, 5.4593)$  and  $\varepsilon_{ij} \sim VM(0, 4.4011)$ . It is worthwhile to note that the variance values of  $\alpha$  and  $\beta$  are small, where  $V\hat{a}r(\hat{\alpha}) = 0.0145$ ,  $V\hat{a}r(\hat{\beta}) = 0.0008$ , this implying the values are close to the mean. Bigger dispersions are obtained for the concentration parameters of the model with values  $V\hat{a}r(\hat{\kappa}_x) = 0.4557$  and  $V\hat{a}r(\hat{\kappa}_y) = 0.2905$  respectively.

## 7. Conclusion

The balance-equal replicated linear functional relationship model with replicated circular variables is proposed in this paper where all the available parameters are derived using the maximum likelihood. According to the Monte Carlo simulation study, parameter estimation provides a good and consistent estimate since the mean of predicted estimation is close to the true value and the bias decreases as the concentration parameter is fixed and the sample size increases. The Variance-Covariance matrix of the estimated parameters can be constructed using various approximations and the Fisher Information matrix.

The model was applied to real data obtained from Holderness Coastline by examining the relationship of wind direction using two separate metrics (HF radar system and anchored wave buoy). It is discovered that the proposed model captures the underlying relationship between the measurement of two circular variables without relying on the ratio of concentration parameter and by replicating the data into balanced and equal replicated data.

## 8. Acknowledgements

The authors would like to express their gratitude to Universiti Pertahanan Nasional Malaysia for providing the space for this study. The authors would like to thank the editors and reviewers for their constructive criticism of this paper.

## 9. References

- Arif, A. M., Zubairi, Y. Z., & Hussin, A. G. (2020a). Nonparametric estimation for a slope of a replicated linear functional relationship model. *ASM Science Journal*, 13, 1–5.
- Arif, A. M., Zubairi, Y. Z., & Hussin, A. G. (2020b). Parameter estimation in replicated linear functional relationship model in the presence of outliers. *Malaysian Journal of Fundamental and Applied Sciences*, 16(2), 158–160.
- Goetz, C., Luo, S., & Stebbins, G. (2019). Modeling the effect of patient's perception of non-motor and motor function on parkinson's disease severity. *Movement Disorder*, 34(Supplement 2), S486–S487.
- Dobson, A. J. (1978). Simple Approximations for the von Mises Concentration Statistic. *Applied Statistics*, 27(3), 345.
- Hannanu, F. F., Goundous, I., Detante, O., Naegele, B., & Jaillard, A. (2020). Spatiotemporal patterns of sensorimotor fMRI activity influence hand motor recovery in subacute stroke: A longitudinal task-related fMRI study. *Cortex*, 129, 80–98.
- Hinton, K., Dang, L., Meyer, F., Villalta-Gil, V., Ganesh, S., Burgess, L., Woodward, N., Landman, B., Lahey, B., & Zald, D. (2018). F82. Latent Factors of Psychopathology and Functional Connectivity of the Dorsal Anterior Cingulate Cortex During Reward Anticipation. *Biological Psychiatry*, 83(9), S269–S270.

- Hussin, A. G., Abuzaid, A., Zulkifili, F., & Ibrahim, M. (2010). Asymptotic Covariance and Detection of Influential Observations in a Linear Functional Relationship Model for Circular Data with Application to the Measurements of Wind Directions. *ScienceAsia*, 36(3), 249–253.
- Hussin, A. G., Fieller, N., & Stillman, E. (2004). Pseudo-replicates in the Linear Circular Functional Relationship Model. *Journal of Applied Sciences*, 5(1), 138–143.
- Kamisan, N. A. B., Hussin, A. G., & Zubairi, Y. Z. (2010). Finding the Best Circular Distribution for Southwesterly Monsoon Wind Direction in Malaysia. *Sains Malaysiana*, 39(3), 387–393.
- Mokhtar, N. A., Zubairi, Y. Z., Hussin, A. G., & Yunus, R. M. (2017). On parameter estimation of a replicated linear functional relationship model for circular variables. *Matematika*, 33(2), 159.
- Moslim, N. H., Mokhtar, N. A., Zubairi, Y. Z., & Hussin, A. G. (2021). Understanding the behaviour of wind direction in Malaysia during monsoon seasons using replicated functional relationship in von mises distribution. *Sains Malaysiana*, 50(7), 2035–2045.
- Satari, S. Z., Hussin, A. G., Zubairi, Y. Z., & Hassan, S. F. (2014). A New Functional Relationship Model for Circular Variables. *Pakistan Journal of Statistics*, 30(3), 387–400.
- Selvaggi, P., Pergola, G., Gelao, B., Di Carlo, P., Nettis, M. A., Amico, G., Fazio, L., Rampino, A., Sambataro, F., Blasi, G., & Bertolino, A. (2019). Genetic variation of a DRD2 co-expression network is associated with changes in prefrontal function after D2 receptors stimulation. *Cerebral Cortex*, 29(3), 1162–1173.